Accepted Manuscript

Journal of the Geological Society

Old detrital AFT ages from E. Greenland do not require plateau erosion

Matthew Fox & Vivi Pedersen

DOI: https://doi.org/10.1144/jgs2023-103

To access the most recent version of this article, please click the DOI URL in the line above. When citing this article please include the above DOI.

Received 27 June 2023
Revised 13 October 2023
Accepted 26 October 2023

Old detrital AFT ages from E. Greenland do not require plateau erosion

Matthew Fox[1], Vivi Pedersen[2]

1 Department of Earth Sciences, University College London, Gower St., London, WC16BT, UK

2 Department of Geoscience, Aarhus University, Høegh-Guldbergs Gade 2, DK-8000 Aarhus, Denmark

Manuscript submitted to

Journal of the Geological Society

*Corresponding author: Matthew Fox

E-mail address: m.fox@ucl.ac.uk

Abstract

Accurate estimates of past topography are required to reliably reconstruct past ice sheets to infer paleoclimate. For this reason, understanding erosion rates across East Greenland is crucial to constrain landscape evolution driven by tectonics and climate-dependent erosion rates. Here we analyse published apatite fission track (AFT) data to constrain the spatial pattern of AFT bedrock ages across the landscape. We compare these bedrock ages with published detrital distribution to highlight ambiguity in the pattern of erosion. In contrast to earlier work, we regress a simple model of exhumation pace through the bedrock ages such that age can vary both as a function of elevation and position. The resulting iso-age surfaces enable us to determine potential source areas for detrital AFT ages distributions. We find that old ages observed in detrital distributions are just as likely to be sourced from low-elevation locations that are far from the coast, as high elevation locations close to the coast. Additional data from lower temperature systems are thus required to make firm conclusions on landscape evolution in the region and distinguish between the two landscape-forming scenarios.

1. Introduction

High-elevation low-relief plateau surfaces separated by deeply incised fjords characterize many high latitude continental margins, including the Antarctic Peninsula, Greenland, and Norway. The origin of this characteristic landscape continues to be debated (e.g., Nielsen et al., 2009; Japsen et al., 2018; Steer et al. 2012; Pedersen et al., 2021), with important implications for understanding long-term glaciation and sea-level. In particular, the dimensions of past glaciations provide a record of paleoclimate but also depend on underlying topography (Kaplan et al., 2009; Anderson et al., 2012; Clague et al., 2002; Sternai et al., 2013). Do the plateau surfaces represent Mesozoic peneplanation and subsequent Cenozoic uplift, or are they formed as a result of glaciation? The former would suggest that the plateau surfaces are eroding very slowly and can be used to map Cenozoic rock uplift, whereas the latter would suggest that they can neither be used to estimate surface uplift nor place constraints on valley incision. In Greenland, studies using cosmogenic nuclides have found that erosion of these high-elevation plateau surfaces has been slow (Strunk et al., 2027; Andersen et al., 2020; Skov et al., 2020), with cosmogenic nuclides abundances preserved and inherited from previous interglacials. However, landscape-evolution modelling efforts have indicated that such observations are in accordance with abundant long-term erosion on the plateau surfaces (Egholm et al., 2017). Indeed, cold-based non-erosive ice at these high-elevation plateau surfaces is an expected consequence of fjord formation that will localize glacial erosion in valley troughs and result in erosion-driven isostatic uplift of the plateau surfaces.

Detrital thermochronometry has the unique potential to reveal where sand is coming from and how this pattern of erosion has changed through time. A recent study by Olivetti et al. (2022) present an impressive detrital AFT data from offshore South and East Greenland (Ocean Drilling Project sites 918 and 987) to provide unique constrains on late Cenozoic erosion across East Greenland. The principle behind this method is that AFT ages record cooling during exhumation through the upper crust and bedrock ages tend to increase with elevation (Wagner, et al., 1979). If the AFT age distribution can be mapped across a bedrock area, detrital AFT ages from glacial

and fluvial sediments can be used as a provenance tool to track patterns of erosion (Hurford and Carter, 1991; Stock and Ehlers, 2006; Vermeesch, 2006; Fox et al., 2015). Detrital AFT ages thus provide an indication of locations being eroded as a function of elevation, with relatively old ages at high elevation (Wagner, et al., 1979). It is this potential that makes the AFT method ideal to determine whether or not the plateau surfaces have been eroding and contributing to detrital material in the late Cenozoic (Garver et al., 1999). Olivetti et al. (2022) highlight that relatively old ages are found in detrital material since 8 million years ago, suggesting prolonged erosion at high elevations. They also argue that even older age populations found in stratigraphic sections closer to the present suggest that progressively higher elevations are contributing detrital material.

However, a few complexities obscure the relationships between bedrock AFT age, elevation, and detrital thermochronometry. First, a single fission track age for a bedrock sample comprises several tens of individual crystal ages (pooled sets of track counts). Pooling of grain data to calculate the pooled fission track age is a means of capturing the stochastic (Poisson) process of fission of U atoms per unit volume. A Poisson distribution for a fission track age will have a standard deviation of single grain ages (counts) thus a single grain age is a single point estimate within the true age distribution. This means that crystals derived from a specific bedrock location will contribute a wide range of single crystal ages to a detrital distribution. Ultimately, this blurs the mapping of detrital age to a specific location (Fox et al., 2015). However, in the case of Greenland, the pooled ages appear to be very consistent as highlighted by the reproducible age-elevation relationships (Olivetti et al., 2022). Second, pooled bedrock AFT ages may not vary as a simple function of elevation. If bedrock age only varies as a function of elevation, surfaces of constant age would be flat and horizontal. These surfaces of constant age are termed iso-age surfaces (Vernon et al., 2008; McPhillips and Brandon, 2010). Spatial variations in bedrock AFT age for a specific elevation may result from spatial variations in exhumation rates as the rocks passed through the AFT closure temperature in the Mesozoic. Spatial variations might also be the result of regional tilting and warping of previously near-horizontal iso-age surfaces. As noted by Olivetti et al., (2022), bedrock AFT ages in East Greenland get progressively older from the coast for the same elevations,

highlighting that ages do not vary simply as a function of elevation. For our purposes, we focus on this second complexity and test whether a simplistic method to predict the bedrock age map limits the conclusions of Olivetti et al., (2022). To do this, however, a new interpolation procedure is required.

To understand the source of sediment and to infer spatial patterns in erosion rate from a detrital dataset, the inferred bedrock age distribution needs to be as accurate as possible. Our aim here is therefore to resolve bedrock age distributions and determine potential source areas for the detrital AFT ages, considering that the distribution of bedrock ages across the East Greenland landscape varies as a function of elevation as well as longitude and latitude. Our approach is based on modelling the slope of the age-elevation relationship in space, under the assumption that the slope of this age-elevation relationship varies smoothly. With this approach, we show that bedrock AFT ages that would yield old detrital AFT ages, are found both across plateau surfaces and in steep parts of the current topography where glacial erosion might be most efficient.

2. Methodology

In the approach we develop here, we regress a spatially-variable model of exhumation pace through elevation-age data using a linear inverse approach. First, we highlight how a single age can be converted to a simple summation equation before we link multiple ages in space. We then apply our approach to available AFT bedrock ages across East Greenland.

A plot of thermochronometric age on the *x*-axis vs elevation on the *y*-axis is commonly referred to as an age-elevation relationship (AER). A linear model regressed through this data has a slope with units of km/Ma, often interpreted as an exhumation rate, and an intercept with units of km, often interpreted as a closure elevation. The closure depth is the difference between the elevation of the sample and the elevation of this closure elevation, which might be below sea level. In contrast, it is convenient to consider this inverse problem as an elevation-age relationship because this ensures that the errors in age are associated with the dependent elevation

variable. The slope of this line is exhumation pace (Ma/km) and the intercept has units of Ma. There are additional benefits of using an EAR over and AER as discussed by Fox and Carter (2020).

Formally we can write that a single age, τ, is the integral of exhumation pace, which varies as function of elevation, *p(z)*, between the elevation of the closure isotherm, h_0, and the elevation of the sample, *h*:

$$\tau = \int_{h_0}^{h} p(z)\,\mathrm{dz} \tag{1}$$

This expression can be discretized into blocks of constant elevation (Δz) and written as a summation equation for a single age:

$$\tau_i = \sum_{j=1}^{M} p_j \Delta z + p_{M+1} z_R \tag{2}$$

where z_R is a remainder term so that the distance between the closure elevation and the sample height (commonly referred to as the closure depth) is $h - h_0 = M\Delta z + z_R$. A similar approach has previously been developed termed GLIDE (Fox et al., 2014a). However, in contrast to GLIDE, we do not calculate the closure depth using a thermal model. Instead, we approach the problem as a geometric problem with the closure depth simply representing a point in elevation. The disadvantage of this is that multiple thermochronometric systems cannot be interpreted simultaneously. An advantage of this is that it reduces the complexity of the model. For example, it is clear that the bedrock ages are the result of a complex thermal history with multiple reheating events (Bernard, et a., 2019; Green et al., 2018). By simply regressing a geometric model, these complex thermal histories can be ignored, and our aim is simply to reproduce the bedrock ages. Furthermore, as we are simply interested in the expected ages at different elevations, we prefer this geometric approach and do not interpret exhumation pace in terms of exhumation rate. We therefore, fix h_0 at a

constant elevation that does not vary in space or time. Because we do not interpret the inferred EAR between this elevation and the lowest elevation ages, this choice does not influence our ability to reproduce the data and predict bedrock ages across the landscape.

A discreet expression, similar to equation 2, can be written for each age in a dataset and these can be combined as a matrix-vector product. If the samples are all from the same location, this solution can be solved with additional constraints to ensure the problem is well-posed. Here the total number of elevation blocks required is determined by the highest elevation sample or M_{max}.

However, if the samples are from different locations, spatial variability is expected. To account for this, we discretize geographic space into a grid of pixels ($N_x * N_y$) with uniform exhumation paces in each pixel and at each position the exhumation pace varies with elevation. Now the total number of unknown exhumation pace parameters is given by $N_x * N_y * M_{max}$. Solving the resulting system of equations requires smoothness constraints. We minimise curvature in space described with the weighting matrix W_s, and curvature in elevation, described with the weighting matrix W_t. These matrices calculate the curvature: across the central pixel and the surrounding 4 pixels for W_s ; and the points above and below for W_t. The relative weights, α and λ, applied to these curvatures are determined using a trial-and-error approach to produce a model that fits the bedrock data. We note that this is potentially an ill-posed inverse problem and multiple combinations of model parameters will fit the data equally well. For this reason, we seek the smoothest model that fits the data and is reasonable. Therefore, we solve:

$$\begin{pmatrix} G \\ W_s \\ W_t \end{pmatrix}(p) = \begin{pmatrix} \tau \\ \mathbf{0} \\ \mathbf{0} \end{pmatrix}. \quad (3)$$

Here the top rows attempt to predict the ages by the spatial variability in exhumation pace. The middle rows ($W_s p = \mathbf{0}$, where $\mathbf{0}$ is a vector of zeros of length $N_x * N_y * M_{max}$) attempt to minimize spatial curvature, and the lower rows ($W_t p =$

$\mathbf{0}$, where $\mathbf{0}$ is a vector of zeros of length $N_x * N_y * M_{max}$) minimize curvature of local EARs.

3. Results

We solve equation 3 for the unknown exhumation pace model using weighting values of α =500 and λ= 10. We use the bedrock data compiled by Olivetti et al., (2022) in this analysis to be consistent with earlier work. In this way, our goal is simply to accurately reproduce the observed bedrock ages and map bedrock ages across the landscape. We do note, however, that areas of our solution will be less reliable than other parts due to the density of surface samples. In particular, in the western limits of our solution, the model is less well constrained and this can be inspected by simply looking at the distance from the bedrock samples. Additional data collected in more locations would improve our interpolation.

Solving equation 3 for the unknown exhumation pace vector, results in a model that matches the observed EARs locally and varies smoothly between these locations (Figure 2). This is in contrast to the maps produced by Olivetti et al. (2022), which cannot honour the observation that multiple ages may be found at the same, or very similar, geographic location (latitude and longitude) due to the fact that age varies as a function of elevation. The most illustrative example of this would result from ages obtained from samples from a truly vertical borehole. Of course, this is an extreme example. In reality, bedrock ages may vary rapidly over short spatial distances, such as with a near vertical profile, and this may obscure any long wavelength trends in the ages. Ignoring this observation and simply mapping age as a function of space, as carried out by Olivetti et al., (2022), means that ages have previously been poorly reproduced by the interpolation procedure. In contrast, the AERs produced by Olivetti et al., (2022), reproduce the local ages perfectly, but do not respect the long-wavelength variability in age. Thus with previous methods it is unclear how representative an AER is of an area and how to combine AER constraints in the spaces between the bedrock sample locations. Our approach allows us to account for long wavelength variation in ages due to underlying geodynamic processes and short wavelength variation due to elevation changes. Furthermore, we are able to reproduce

the bedrock ages and predict ages at all surface locations. An ability to predict ages at all surface locations is a requirement because the detrital ages integrate bedrock data across space.

The exhumation pace maps are relatively stable through elevation except where changes in the slope of the AER have previously been detected. We show three representative maps here (Figure 3). We stress that these maps should not be interpreted in terms of an exhumation rate history because the exhumation pace parameters do not constrain exhumation rate over the same time intervals. Furthermore, we have not accounted for the topographic effects on the elevation of the closure isotherm or changes in the advection of heat due to exhumation. At high elevations, the pace maps show relatively high pace, slow rate, across most of the area. At lower elevations, the pace maps show lower values towards the south.

Finally, we can predict age as a function of elevation and geographic position. To do this we solve equation 2 for each elevation point in a DEM using the recovered exhumation pace from our analysis of the bedrock data. Figure 4 shows topography (A), topographic slope (B) and predicted age (C). We see that old ages are found at high elevations and further from the coast, in agreement with earlier work. However, here we are able to interpolate and extrapolate between datapoints because of the simplicity of the model.

4. Discussion

Olivetti et al. (2022) argued that the old age populations they found within offshore detrital samples indicate that the high-elevation plateau surfaces are producing detrital material as far back as 8 Ma. This is contentious because it raises the question of whether these are formed *in situ* or can be used to map uplift of a low-relief surface in space. We can highlight that the old ages might simply be coming from high slope parts of the landscape simply by hiding parts of Figure 4 that have ages that would not contribute to this old population. We define a mask as ages between 250 and 300 Ma. This corresponds to the "old" age population identified by Olivetti et al., (2022). Figure 5 shows that the old population could correspond to both high and low

elevations (Figure 5A), as well as low and high slope areas (Figure 5C). This is consistent with the idea that sediment is produced where glaciers are sliding fastest (Herman et al., 2015). Indeed, to determine where the sediment is coming from, additional data is required.

It is also possible to estimate the probability of erosion based on the distribution of detrital ages and the bedrock maps. To do this, we fit a kernel density estimate through the detrital ages which is proportional to probability (Vermeesch, 2012). Here we use the youngest detrital sample from the Site 987, which has a depositional age of 0.7±0.1 Ma (Figure 6A). We then map the age probabilities onto the landscape to produce a simple map of probability of erosion (Figure 6B). The most striking feature of this map is the high probability of erosion from very low elevations that are below sea level. These are highlighted by the red colours at low elevations. This is challenging to explain in terms of modern erosional processes because we would expect the base of deep glacial fjords to be depositional environments. However, given that this sample is from sediment deposited at 0.7 Ma it makes sense that the high probability of erosion in the base of the fjords could be the result of glacial erosion and deepening when glaciers occupied the fjords (Sternai et al., 2013; Pedersen et al., 2014; Fox et al., 2014b). Interestingly, high erosion probability values are predicted within the over-deepened fjord even during these late stages of glaciation, whereas it might be expected that the focus of erosion would migrate headwards through time (Shuster et al., 2011). We also see high probabilities of erosion across higher elevations parts of the catchment that are potentially incising where old bedrock ages are found. This is more consistent with the hypothesis that valley erosion would migrate headwards through time. Across the high-elevation low-relief surfaces, we mostly see low probability of erosion.

Bedrock ages with different spatial patterns would be required to leverage the detrital dataset to determine whether old ages are coming from low-relief high elevation surfaces or incising valleys. In this way, the production function (where sediment is coming from) is the same but the bedrock age function is different. The apatite (U-Th)/He system with a lower closure temperature would be ideal because the ages will be controlled by topographic evolution as opposed to earlier tectonic events.

Furthermore, radiation damage influences the closure temperature of this system so that damaged crystals have higher closure temperatures than less damaged crystals. With sufficient data, the apatite (U-Th)/He system combined with radiation damage effectively provides a suite of slightly different thermochronometric systems. Therefore, a specific detrital age fingerprints different locations depending on the amount of radiation damage. Physically based models accounting for heat flow, topographic evolution and damage would be required for this sort of analysis (Clinger et al., 2020; Clinger et al., 2022). Furthermore, accounting for these complexities, along with collecting additional data, would allow additional processes to be investigated. These include whether sediment is mixed during glacial transportation (Bernard et al., 2020), how lithology influences glacial erosion (Bernard et al., 2021) or how overdeepened basins trap sediment and nutrients (Delaney and Adhikari, 2020; Swift et al., 2021; Cook and Swift, 2012).

By interpreting bedrock data with simple tools to map age as a function of space, the bedrock age distribution can be interpolated and extrapolated. We note that aspects of our model, particularly towards the west, may be poorly resolved due to large distances between bedrock ages. Ultimately, the only way to improve this is to collect additional bedrock data. We have used a geometrical model because we simply want to reproduce the bedrock age distribution, but models that solve heat transport could also be used. Either way, earlier simplistic models relating age to elevation may yield conclusions that are dependent on a model that is too unrealistic.

Our ability to estimate the source locations of sediment offshore of inaccessible locations has important implications for understanding landscape evolution. If the low-relief surfaces are not eroding and have not been eroding over the last 8 Ma, as suggested by our analysis, these surfaces can be used to estimate the magnitudes of valley incision and patterns of geodynamic processes. This also implies that glaciers in Greenland have cut deep fjords into a relatively low-relief landscape that existed prior to glaciation. Ultimately, such a reconstructed low-relief landscape could be used to simulate glacial conditions at the time of glacial inception with improved fidelity.

5. Summary

We have shown that the current combination of bedrock AFT data and detrital AFT data cannot determine whether the low-relief, high elevation surfaces of Greenland have been eroding for the last 8 Ma. By interpolating a simple model through available data, we are able to predict bedrock data and extrapolate the exhumation pace between data points. Resulting predicted bedrock AFT ages highlight that old ages are found in low-elevation and relatively steep parts of the landscape, in addition to the high-elevation plateau surfaces that have previously been put forward as their source. At these locations, ice is expected to be thick and fast flowing potentially producing high rates of glacial erosion. Propagating uncertainties from the measured ages, interpolation model, and detrital distributions would simply make conclusions drawn from the data less discriminating and this is not required here.

Acknowledgements

We would like to thank Valerio Olivetti for sharing the detrital dataset and providing helpful comments on the manuscript. This work was supported by NERC (NE/N015479/1).

References

Anderson, R.S., Dühnforth, M., Colgan, W. and Anderson, L., 2012. Far-flung moraines: Exploring the feedback of glacial erosion on the evolution of glacier length. Geomorphology, 179, pp.269-285.

Andersen, J.L., Egholm, D.L., Knudsen, M.F., Linge, H., Jansen, J.D., Pedersen, V.K., Nielsen, S.B., Tikhomirov, D., Olsen, J., Fabel, D. and Xu, S., 2018. Widespread erosion on high plateaus during recent glaciations in Scandinavia. Nature Communications, 9(1), pp.830.

Andersen, J.L., Egholm, D.L., Olsen, J., Larsen, N.K. and Knudsen, M.F., 2020. Topographical evolution and glaciation history of South Greenland constrained by paired 26Al/10Be nuclides. Earth and Planetary Science Letters, 542, pp.116300.

Bernard, T., Steer, P., Gallagher, K., Szulc, A., Whitham, A. and Johnson, C., 2016. Evidence for Eocene–Oligocene glaciation in the landscape of the East Greenland margin. Geology, 44(11), pp.895-898.

Bernard, M., Steer, P., Gallagher, K., & Egholm, D. L., 2021. The impact of lithology on fjord morphology. Geophysical Research Letters, 48(16), e2021GL093101.

Bernard, M., Steer, P., Gallagher, K., & Egholm, D. L., 2020. Modelling the effects of ice transport and sediment sources on the form of detrital thermochronological age probability distributions from glacial settings. Earth Surface Dynamics, 8(4), 931-953.

Clinger, A.E., Fox, M., Balco, G., Cuffey, K. and Shuster, D.L., 2020. Detrital thermochronometry reveals that the topography along the Antarctic Peninsula is not a Pleistocene landscape. Journal of Geophysical Research: Earth Surface, 125(6), p.e2019JF005447.

Clinger, A., Fox, M., Balco, G., Cuffey, K. and Shuster, D., 2022. Tectonic controls on the timing of fjord incision at the Antarctic Peninsula. Earth and Planetary Science Letters, 585, pp.117528.

Clague, J.J., Barendregt, R.W., Menounos, B., Roberts, N.J., Rabassa, J., Martinez, O., Ercolano, B., Corbella, H. and Hemming, S.R., 2020. Pliocene and Early Pleistocene glaciation and landscape evolution on the Patagonian Steppe, Santa Cruz province, Argentina. Quaternary Science Reviews, 227, pp.105992.

Cook, S. J., & Swift, D. A., 2012. Subglacial basins: Their origin and importance in glacial systems and landscapes. Earth-Science Reviews, 115(4), 332-372.

Delaney, I., & Adhikari, S., 2020. Increased subglacial sediment discharge in a warming climate: Consideration of ice dynamics, glacial erosion, and fluvial sediment transport. Geophysical Research Letters, 47(7), e2019GL085672.

Egholm, D.L., Jansen, J.D., Brædstrup, C.F., Pedersen, V.K., Andersen, J.L., Ugelvig, S.V., Larsen, N.K., and Knudsen, M.F., 2017, Formation of plateau landscapes on glaciated continental margins: Nature Geoscience, v. 10, p. 592–597, https://doi .org/10.1038/ngeo2980.

Fox, M. and Carter, A., 2020. Heated topics in thermochronology and paths towards resolution. Geosciences, 10(9), pp.375.

Fox, M., Leith, K., Bodin, T., Balco, G. and Shuster, D.L., 2015. Rate of fluvial incision in the Central Alps constrained through joint inversion of detrital 10Be and thermochronometric data. Earth and Planetary Science Letters, 411, pp.27-36.

Fox, M., Herman, F., Willett, S.D. and May, D.A., 2014a. A linear inversion method to infer exhumation rates in space and time from thermochronometric data. Earth Surface Dynamics, 2(1), pp.47-65.

Fox, M., Reverman, R., Herman, F., Fellin, M.G., Sternai, P. and Willett, S.D., 2014b. Rock uplift and erosion rate history of the Bergell intrusion from the inversion of low temperature thermochronometric data. Geochemistry, Geophysics, Geosystems, 15(4), pp.1235-1257.

Garver, J.I., Brandon, M.T., Roden-Tice, M. and Kamp, P.J., 1999. Exhumation history of orogenic highlands determined by detrital fission-track thermochronology. Geological Society, London, Special Publications, 154(1), pp.283-304.

Green, P.F., Japsen, P., Chalmers, J.A., Bonow, J.M. and Duddy, I.R., 2018. Post-breakup burial and exhumation of passive continental margins: Seven propositions to inform geodynamic models. Gondwana Research, 53, pp.58-81.

Herman, F., Beyssac, O., Brughelli, M., Lane, S.N., Leprince, S., Adatte, T., Lin, J.Y., Avouac, J.P. and Cox, S.C., 2015. Erosion by an Alpine glacier. Science, 350(6257), pp.193-195.

Hurford, A.J. and Carter, A., 1991. The role of fission track dating in discrimination of provenance. Geological Society, London, Special Publications, 57(1), pp.67-78.

Kaplan, M.R., Hein, A.S., Hubbard, A. and Lax, S.M., 2009. Can glacial erosion limit the extent of glaciation?. Geomorphology, 103(2), pp.172-179.

McPhillips, D. and Brandon, M.T., 2010. Using tracer thermochronology to measure modern relief change in the Sierra Nevada, California. Earth and Planetary Science Letters, 296(3-4), pp.373-383.

Morlighem, M. et al., 2017. IceBridge BedMachine Greenland, Version 3 [Data Set]. Boulder, Colorado USA. NASA National Snow and Ice Data Center Distributed Active Archive Center. https://doi.org/10.5067/2CIX82HUV88Y.

Olivetti, V., Cattò, S. and Zattin, M., 2022. Increased erosion of high-elevation land during late Cenozoic: evidence from detrital thermochronology off-shore Greenland. Scientific Reports, 12(1), p.9932.

Pedersen, V.K., Knutsen, Å.R., Pallisgaard-Olesen, G., Andersen, J.L., Moucha, R. and Huismans, R.S., 2021. Widespread glacial erosion on the Scandinavian passive margin. Geology, 49(8), pp.1004-1008.

Pedersen, V.K., Huismans, R.S., Herman, F. and Egholm, D.L., 2014. Controls of initial topography on temporal and spatial patterns of glacial erosion. Geomorphology, 223, pp.96-116.

Shuster, D.L., Cuffey, K.M., Sanders, J.W. and Balco, G., 2011. Thermochronometry reveals headward propagation of erosion in an alpine landscape. Science, 332(6025), pp.84-88.

Skov, D. S. et al. Constraints from cosmogenic nuclides on the glaciation and erosion history of Dove Bugt, northeast Greenland. Geol. Soc. Am. Bull. 132, 2282–2294 (2020).

Steer, P., Huismans, R.S., Valla, P.G., Gac, S. and Herman, F., 2012. Bimodal Plio–Quaternary glacial erosion of fjords and low-relief surfaces in Scandinavia. Nature Geoscience, 5(9), pp.635-639.

Sternai, P., Herman, F., Valla, P.G. and Champagnac, J.D., 2013. Spatial and temporal variations of glacial erosion in the Rhône valley (Swiss Alps): Insights from numerical modeling. Earth and Planetary Science Letters, 368, pp.119-131.

Stock, G.M., Ehlers, T.A. and Farley, K.A., 2006. Where does sediment come from? Quantifying catchment erosion with detrital apatite (U-Th)/He thermochronometry. Geology, 34(9), pp.725-728.

Strunk, A., Knudsen, M.F., Egholm, D.L., Jansen, J.D., Levy, L.B., Jacobsen, B.H., Larsen, N.K., 2017. One million years of glaciation and denudation history in west Greenland. Nat. Commun.8, 14199.

Swift, D. A., Tallentire, G. D., Farinotti, D., Cook, S. J., Higson, W. J., & Bryant, R. G., 2021. The hydrology of glacier-bed overdeepenings: Sediment transport mechanics, drainage system morphology, and geomorphological implications. Earth Surface Processes and Landforms, 46(11), 2264-2278.

Vernon, A.J., Van Der Beek, P.A., Sinclair, H.D. and Rahn, M.K., 2008. Increase in late Neogene denudation of the European Alps confirmed by analysis of a fission-track thermochronology database. Earth and Planetary Science Letters, 270(3-4), pp.316-329.

Vermeesch, P., 2007. Quantitative geomorphology of the White Mountains (California) using detrital apatite fission track thermochronology. Journal of Geophysical Research: Earth Surface, 112(F3).

Vermeesch, P., 2012. On the visualisation of detrital age distributions. Chemical Geology, 312, pp.190-194.

Wagner, G.A., Miller, D.S. and Jäger, E., 1979. Fission track ages on apatite of Bergell rocks from central Alps and Bergell boulders in Oligocene sediments. Earth and Planetary Science Letters, 45(2), pp.355-360.

Figures

Figure 1. Greenland topography and bedrock data. A) Digitial Elevation Model (Morlighem et al., 2017) of Greenland showing the sample locations. The detrital sample is from a location just to the east of the map extents. The black box shows the location of Figure 3, 4 and 5. The potential source area is hard to define because ice can flow over topographic divides, but we expect it covers much of the study area.

Figure 2. Greenland data and predictions. A) The relationship between actual age and predicted age for the dataset analysed. Most of the data fall on the 1:1 line indicating that the model fts the data. B) Age-elevation relationships for the data and model predictions. The data are shown as open circles and the predictions are shown as stars. The model has the flexibility to reproduce most of the ages. Importantly, we do not wish to fit all the data perfectly because then we are unable to average out noise and errors.

Figure 3. Exhumation pace for three different elevation intervals. A) B) and C). An exhumation pace of 0.01 Ma/m is equivalent to 0.1 km/Ma, for example. Two parameters influence the smoothness of the maps. Geographic smoothness is controlled by α, so that large values force planar iso-age surfaces and small values provide no ability to interpolate between sample locations. EAR complexity is controlled by λ, so that large values force straight EARs with no breaks-in-slope, whereas small values allow rapid changes in the slope of the EAR but no ability to account for noise. Pixel sizes are 10 x 10 km and the vertical discretization is 250 m.

We use a value of α of 500 and a value of λ of 10 as this provides a reasonable compromise between these two weighting terms and provides a good fit to the data (Figure 2). The black dots are the bedrock sample locations.

Figure 4. Characteristics of the catchment area. A) Bedrock elevation showing deep glacial fjords and low-relief, high elevation surfaces. B) Age map calculated by solving equation 3 for the bedrock elevation and inferred exhumation pace function. C) Slope map showing where the topography is steep and where it is low. It might be expected that glacial erosion is focussed in glacial valleys where slopes are high.

Figure 5. Characteristics of the topography where old ages are found. This is a reproduction of Figure 4 and simply highlights the geomorphology of the areas where old ages are found. A) Many of the deepest fjords are hidden highlighting that these locations do not contribute to the 'old' population of detrital ages. B) Old ages are found across varying geomorphic domains: at high elevations and in the deeper valleys that cut into the low-relief surface at high elevations. C) Slope map showing that old ages are found in locations with high slope.

Figure 6. The probability of bedrock ages contributing to the detrital distribution. A) Detrital ages from sample 987B_9H5 from Olivetti et al. (2022). The black line shows a kernel density estimate and this is proportional to probability. B) Map of probability that a location contributes ages to the detrital population. This is a function of the bedrock age distribution and the detrital distribution. High probabilities are found below sea level suggesting that glacial erosion during the LGM might be responsible for producing some of the detrital material. Low probabilities are observed on the low-relief high-elevation surfaces.

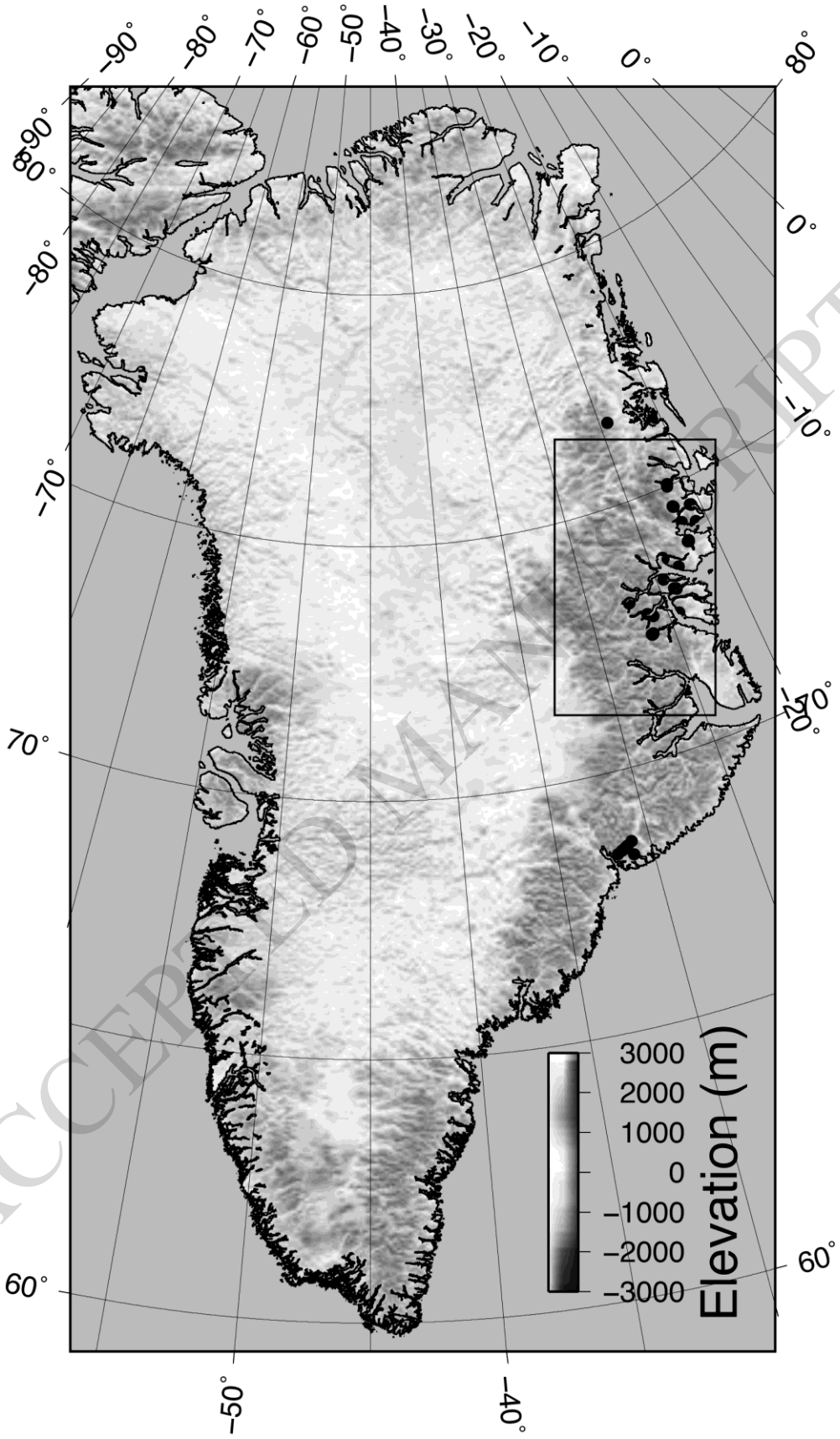

Figure 1

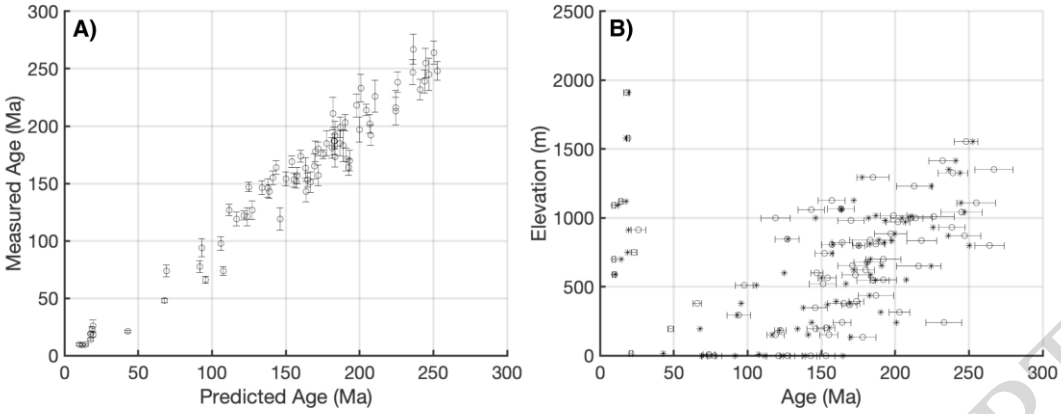

Figure 2

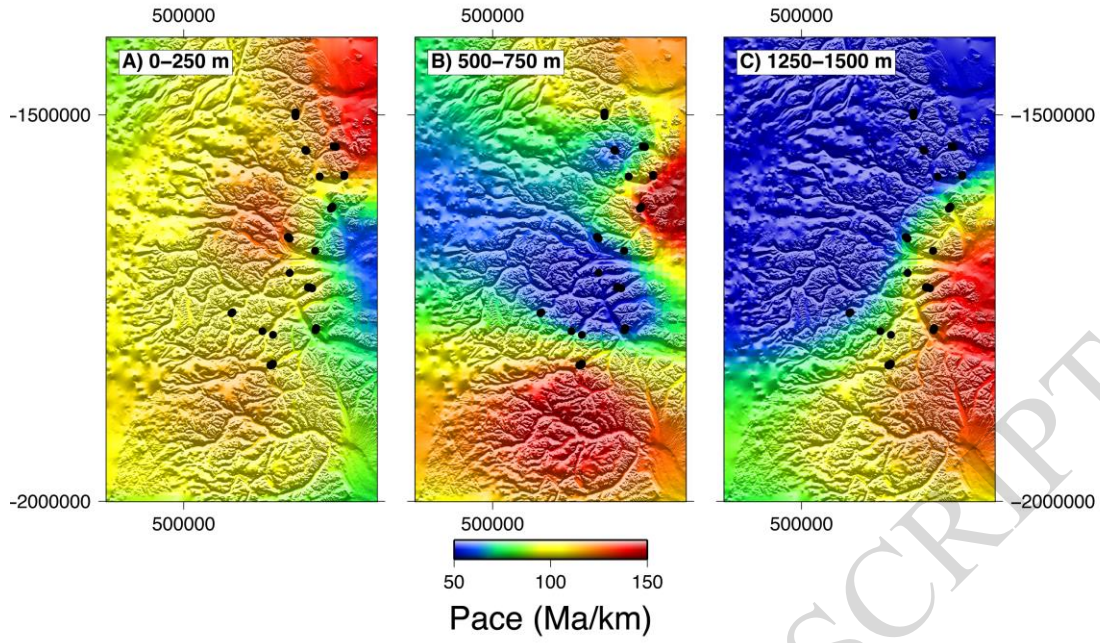

Figure 3

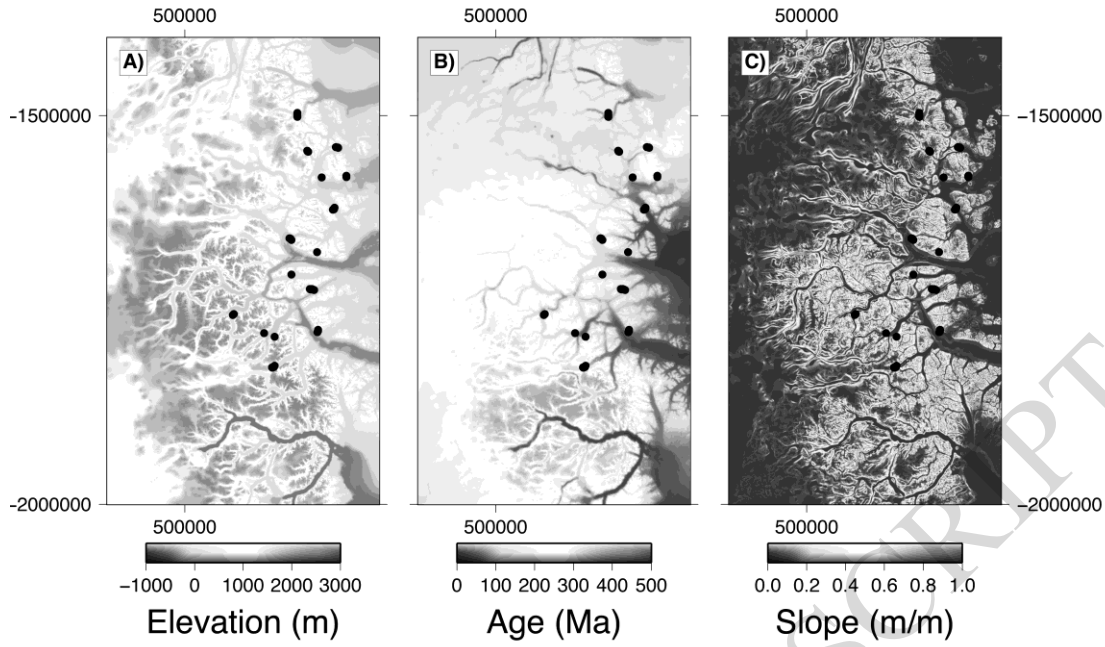

Figure 4

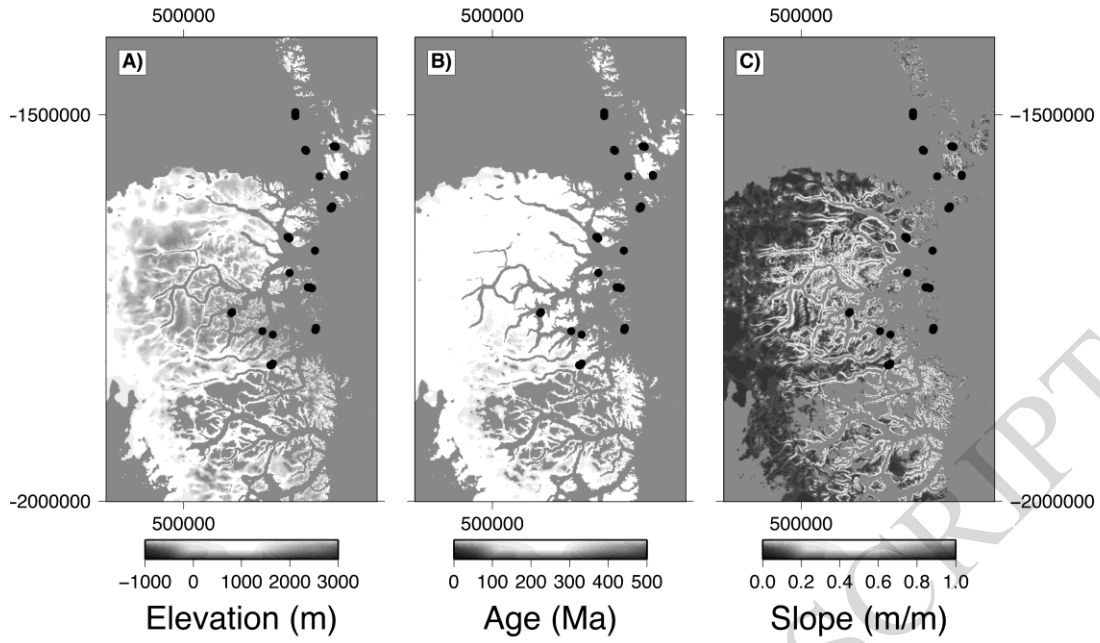

Figure 5

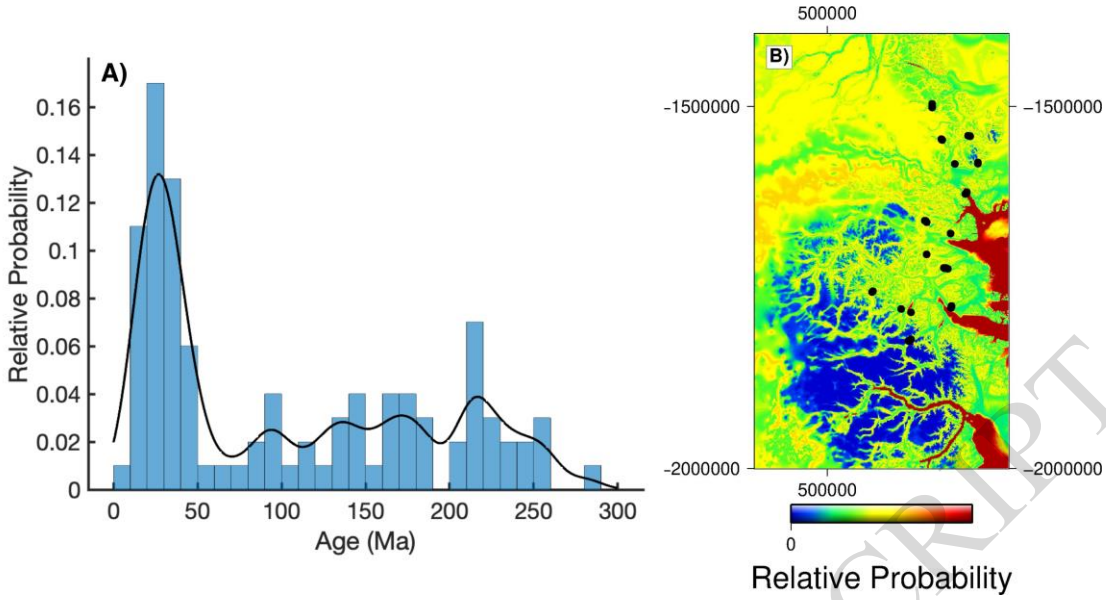

Figure 6